Journal of Chromatography A, 1228 (2012) 72–88

Contents lists available at ScienceDirect

Journal of Chromatography A

journal homepage: www.elsevier.com/locate/chroma

Applications of superficially porous particles: High speed, high efficiency or both?

Xiaoli Wang*, William E. Barber, William J. Long

Agilent Technologies, Inc., 2850 Centerville Road, Wilmington, DE 19808, USA

ARTICLE INFO

Article history:
Available online 30 July 2011

Keywords:
Superficially porous particles
Applications
Separation efficiency
Separation speed
Optimization

ABSTRACT

The new generation of superficially porous particles (SPPs) offers impressive chromatographic efficiency compared to totally porous particles. Specifically, modern sub-3-μm SPPs generate much improved reduced plate height but at lower backpressure compared to sub-2-μm totally porous particles. This feature makes them attractive for various types of applications and SPPs are quickly being adopted in many analytical laboratories. In this review, we use optimization theory to compare the performance limit of modern SPPs and totally porous particles under optimized conditions, in order to answer the question: what are the optimal applications for modern SPPs? Are they most suitable for fast separations, or for high efficiency separations, or for both? Successful examples of using modern SPPs in different application areas are reviewed, over a wide range of sample complexity and analysis time. Practical aspects of the use of such particles and future development possibilities are also discussed.

1. Introduction

Superficially porous particles (SPPs) are different from the more commonly used totally porous particles in that they have a solid core surrounded by a thin porous shell. They are also referred to as fused-core, shell or core–shell particles. The initial intention of designing such particle structure was to reduce the analyte diffusion length inside the particle while not increasing column backpressure at a given eluent velocity. The development of these materials started four decades ago when Horvath and Lipsky made very large pellicular particles for ion-exchange separations [1]. Since then, such particles have gone through several cycles of active and stagnant development [2]. The major breakthrough in this technology occurred in 2006 when Kirkland et al. commercialized the modern sub-3-μm superficially porous particles, whose success revitalized research interest in such particle design. Currently sub-3-μm and sub-2-μm superficially porous particles are available from several manufacturers. These include Halo from Advanced Material Technologies, Kinetex from Phenomenex, and Poroshell 120 from Agilent Technologies. The list of commercially available superficially porous particles continues to grow as evident from recent conference proceedings [3].

Due to their exceptional chromatographic efficiency, modern superficially porous particles are quickly gaining popularity in analytical labs [4]. Another factor that helped their quick adoption was that such particles could be used on traditional HPLC equipment with careful instrument optimization, although the trend of moving to ultrahigh pressure LC seems inevitable in the next decade [5]. With the increasing number of users, more and more applications are being developed on the modern superficially porous particles. Some applications meet analysts' needs for faster separations, and some for resolving challenging samples.

The history, physico-chemical properties and chromatographic performance of superficially porous particles are discussed in a recent comprehensive and fundamental review by Guiochon et al. [2]. They focused on discussing the kinetic properties and mass transfer mechanism in columns packed with such particles. In this article, we intend to use optimization theory with these column characteristics as inputs to study the performance potential of modern superficially porous particles. Specifically we look at the two most practically important metrics of separation, i.e. efficiency as measured by plates and speed as measured by plates per unit time, in order to answer the question: are the modern superficially porous particles most suitable for fast separations, or for high efficiency separations, or for both? We then review successful applications in the literature and discuss the practical considerations when using such particles and future development possibilities. For simplicity, we refer to superficially porous particles as SPPs in the rest of this paper.

2. Need for faster or more efficient separations

Different applications require different separations. Some applications require high speed but not high resolution, while some

* Corresponding author. Tel.: +1 302 636 1946; fax: +1 302 636 1585.
E-mail address: xiaoli_wang@agilent.com (X. Wang).

0021-9673/$ – see front matter © 2011 Elsevier B.V. All rights reserved.
doi:10.1016/j.chroma.2011.07.083

Nomenclature

N	plate count
h	reduced plate height
ν	reduced interstitial linear velocity
d_p	particle size (μm)
L	column length (mm)
u_e	interstitial linear velocity (cm/s)
D_m	diffusion coefficient (cm^2/s)
A, B, C	van Deemter equation coefficients
t_0	Column dead time (s)
ρ	ratio of core diameter and total particle diameter
ε_e	interstitial porosity
ε_p	intra-particle porosity
ε_t	total porosity of a column
P	pressure (bar)
ϕ	flow resistance based on interstitial velocity
η	mobile phase viscosity
λ	ratio of interstitial porosity and total porosity
A_{sp}	specific surface area (m^2/g)
b	gradient steepness
t_G	gradient time
V_m	column dead volume
Δc	change in eluent strength during a gradient elution
F	flow rate
S	slope of solute retention $\ln k'$ vs. eluent strength

applications require high resolution but not high speed. This is largely dependent on the sample complexity. Fig. 1 shows where most common applications fit in the space of efficiency (i.e. plates) vs. analysis time. These applications line up on the diagonal line of the graph, clearly suggesting the compromise between plates and time [6]. The high speed and high efficiency region are ideal but unfortunately inaccessible, and as a result, one has to sacrifice plates for time or vice versa. In this section, we discuss the optimum applications for SPPs from a theoretical perspective, focusing on the most common analysis times between 1 and 100 min (or column dead time between 10 and 1000 s assuming a k' of 5).

2.1. Characteristics of modern superficially porous particles

The characteristics of the new generation SPPs are briefly summarized here for discussion purposes. For further details, the reader is referred to the comprehensive review of Guiochon et al. [2].

2.1.1. Physico-chemical properties

The most notable physical property of SPPs is their very narrow particle size distribution (PSD), with a d90/d10 of less than 1.20, compared to typical values of 1.3–2.0 for totally porous particles. This is due to the fact that the Stöber process used to make the solid cores [7] is known to give a narrow PSD, which is maintained during the subsequent process of building the thin porous shell. It has been hypothesized that the narrow PSD reduces eddy dispersion of packed columns, thus contributing to the exceptional efficiency obtained on SPPs [8–10]. However, this hypothesis continues to be debated and actually contradicts with some observations on the effect of the PSD on performance of columns packed with totally porous particles [11,12].

Performance of SPPs depends on the properties of the porous shell, including the shell layer thickness and volume fraction, pore size and pore structure. For example, the ratio of the core diameter and total particle diameter (ρ) varies from 0.63 to 0.74 for different modern SPPs. This ratio is critical to understanding the effect of reducing the intra-particle diffusion length of analytes while maintaining the column permeability. The volume fraction of the shell ($1-\rho^3$) varies from 75% to 60% and this largely determines the sample loading capacity compared to totally porous counterparts. The pore size and pore structure are strongly affected by the manufacturing process used to build the porous layer, such as layer-by-layer coating and coacervation. The commercially available average pore size varies from 90 Å to 120 Å for small molecule applications and was recently extended to 160 Å for peptide applications [13,14]. Despite all these differences, the chromatographic efficiency of different modern SPPs is consistently better than totally porous particles, in that they all provide much improved reduced HETP when packed into 4.6 mm i.d. columns (1.5 or lower vs. 2.0 or higher).

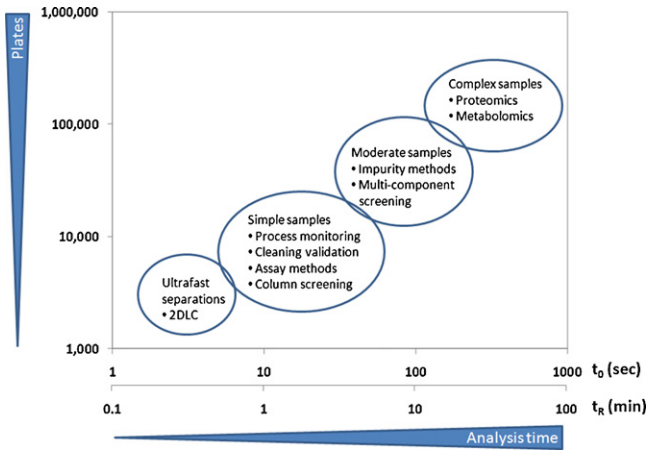

Fig. 1. Compromise of speed vs. efficiency for different applications. The *X*-axis is either column dead time in seconds, or analysis time in minutes assuming an isocratic k' of 5. The *Y*-axis is the plate count.

2.1.2. Chromatographic performance

The mass transfer kinetics of modern SPPs were studied extensively by Guiochon and co-workers to understand the improved HETP compared to totally porous materials [2,15,16]. The key mass transfer terms that contribute to the overall HETP are eddy dispersion, longitudinal diffusion, and resistance to mass transfer (including both intra-particle and external film contributions).

The eddy dispersion term of SPPs can be as much as 40% smaller than that of totally porous particles for 4.6 mm i.d. columns and this contributes most to the improvement in h_{min}. This could be due to the narrower PSD of SPPs. Gritti et al. also suggested that the surface roughness of SPPs might lead to a more homogeneous packed bed, which might reduce the trans-column eddy dispersion term [2]. Unfortunately, few results are available to allow unambiguous conclusions. It is important to note that narrow-bore columns packed with SPPs have significantly higher h_{min} and thus a larger eddy dispersion term [17]. This is certainly an area that needs to be addressed more completely as solvent efficient narrow-bore columns have already become mainstream for 'greener' chromatography.

Another reason for the superior performance of SPPs is the reduced longitudinal diffusion term, primarily due to the smaller particle porosity caused by the solid core. This has been observed experimentally; the van Deemter B terms for SPPs are 30–50% smaller than those for totally porous particles [2,10,18,19]. A recent theoretical study also suggests that B term contributions up to 33% lower are expected for SPPs vs. totally porous particles, assuming they have the same pore structure [20,21]. However, the smaller B term has a relatively small effect on overall HETP when flow rate is at the van Deemter optimum or higher (<0.2 h unit). Instead the benefit of a smaller B term becomes important when columns are operated at low flow rate, as in the case of using coupled columns

to achieve ultrahigh efficiency with a fixed particle size, see Eq. (7) [19,22,23].

Interestingly, for small molecules the overall C term of SPPs is similar to that of totally porous particles [2,10]. This is unexpected since the initial intent in developing SPPs was to reduce the intra-particle diffusion distance, thereby reducing the internal mass transfer resistance. Gritti et al. studied this in detail and conclude that the dominant contribution to the overall C term was the external film mass transfer resistance (C_f), not the intra-particle mass transfer resistance (C_p), at least for small molecules. For larger molecules like proteins, the apparent C terms of different SPPs differ substantially, but primarily due to the different pore sizes, thus offering different accessible pore volumes to the analyte [15].

2.2. Theoretical considerations

Given the known properties of modern SPPs, we can use theory to assess their performance potential and to predict their optimal applications. As summarized in a recent paper, there are three types of optimization in HPLC method development with different levels of complexity [24]. The simplest approach is one-parameter optimization, where only the flow rate (linear velocity) is varied on a fixed column (i.e. fixed particle size and column length) by using the van Deemter equation. A more useful approach is two-parameter optimization, where both flow rate and column length are varied with a fixed particle size. This can be achieved by using the "Poppe plot" or kinetic plots [25,26]. The most sophisticated but ideal approach is three-parameter optimization, where flow rate, column length and particle size are simultaneously varied. This approach predicts the combination of parameters that will lead to the best possible separation at a given pressure limit and required analysis time.

In this section, we use these theories to compare four types of particles. Monolith is not included here and discussion on its performance can be found in the literature [27,28].

1. Sub-3-μm SPPs. These are the most popular modern SPPs and can typically be operated up to 600 bar. They are available in various column i.d. such as 4.6, 3.0 and 2.1 mm.
2. Sub-2-μm SPPs. These smaller SPPs can be operated at ultrahigh pressure (e.g. 1000 bar). They are available in 2.1 or 3.0 mm i.d. columns.
3. Sub-2-μm totally porous particles. These are the finest totally porous particles that were developed for ultrahigh pressure separations and are mainstream for UHPLC. They are typically available in narrow-bore columns such as 2.1 or 3.0 mm i.d.
4. Traditional totally porous particles. These are the most popular totally porous particles for HPLC applications, with particle sizes from 2.5 to 5 μm. Commercial columns packed with such particles are available in various column i.d. such as 4.6, 3.0 and 2.1 mm, and are typically rated up to 400 bar due to the limitation of column hardware. However, in this work, we use the same operating pressure limit of 600 bar as the sub-3-μm SPPs in our calculation. This allows us to focus on studying the effect of particle type and particle size.

Table 1 lists the column characteristics that we selected based on literature results and they are representative for each type of particle [2,10,19,29]. Clearly particles from different column vendors behave differently [2]. Therefore, the selection of these values is not meant to compare specific brands. Instead they are used to provide a general comparison between the performances of different types of particles. Interested readers should use the exact calculation results in this section with caution for their method development.

Since the column characteristics strongly affect calculation results, the rationale for their selection warrants some discussion.

1. Columns packed with SPPs have larger interstitial porosities compared to those packed with totally porous particles [15]. This may be due to the rougher surface of SPPs which causes more friction between particles during column packing and thus leads to a less densely packed bed. The interstitial porosities are chosen as 0.40 and 0.38 for SPPs and totally porous particles, respectively.
2. SPPs have lower intra-particle porosity. Values of 0.20 and 0.30 are selected for SPPs and totally porous particles, respectively, based on reported results for C18 bonded particles [10].
3. It is unclear if the higher interstitial porosity of the SPPs leads to lower flow resistance. Our own measurements and some literature suggest that the flow resistance is similar between columns packed with SPPs and totally porous particles [10]. Therefore a value of 450 is selected for all four particles.
4. The B coefficients are selected as 4.5 and 7.0 for SPPs and totally porous particles, respectively. They represent typical values for a compound with k' about 5, based on results found in the literature [10,19].
5. Many authors reported that the C term of SPPs for small molecules is similar to that of totally porous particles [2,10,18]. Thus a representative value of 0.04 is selected for a compound with k' about 5.
6. Based on literature values [2,10], the minimum HETPs are chosen as 1.5, 2.2, 2.2, and 2.0 for sub-3-μm SPPs, sub-2-μm SPPs, sub-2-μm totally porous and traditional totally porous particles, respectively. The higher HETPs for the sub-2-μm particles likely reflect the difficulty in packing such materials into narrow-bore columns.
7. The A terms for the four particles are adjusted in order to reach the minimum HETP values listed above.

It is important to note that the A, B and C terms here are apparent coefficients of van Deemter equations from least square fitting. The absolute values are different from those obtained from theoretical modeling as done by Gritti et al. However, careful selection of these values is required for subsequent theoretical calculations, which allow us to accurately reproduce experimental HETP vs. velocity curves, and this is ultimately what matters for chromatographic performance.

Next, we use theory with these column characteristics as inputs to compare the different types of particles, and predict the optimal applications for each particle type. We focus on three common types of separations:

1. Ultrafast separations with 1-min analysis time (column dead time being 10-s assuming a k' of 5). Such separations are good for applications such as quick assays, process monitoring and cleaning validation.
2. Common separations with 10-min analysis time (column dead time being 100-s assuming k' of 5). Such separations are good for moderately complex samples such as impurity methods.
3. Ultrahigh efficiency separations with 100-min analysis time (column dead time being 1000-s assuming k' of 5). Such separations are good for complex samples, including proteomic and metabolomic analysis.

2.2.1. Three-parameter optimization

Ideally one would like to simultaneously vary particle size, column length and flow rate to obtain the best separation. An important assumption in such optimization is that the column characteristics are independent of particle size, which may not be

Table 1
Column characteristics selected for four different types of particles.

Properties	Sub-3-μm SPPs	Sub-2-μm SPPs	Sub-2-μm totally porous	Traditional totally porous
Typical particle size (μm)	2.6–2.7	1.7	1.7–1.9	2.5–5.0
Maximum pressure (bar)	600	1000	1000–1200	600
ε_e (interstitial porosity)	0.40	0.40	0.38	0.38
ε_p (intra-particle porosity)	0.20	0.20	0.30	0.30
ε_t (total porosity)	0.52	0.52	0.57	0.57
ϕ (flow resistance)[a]	450	450	450	450
van Deemter *A* term[b]	0.65	1.30	1.10	0.95
van Deemter *B* term[b,c]	4.5	4.5	7.0	7.0
van Deemter *C* term[c]	0.04	0.04	0.04	0.04
h_{min} (minimum HETP)	1.50	2.15	2.16	2.01
ν_{opt} (optimum velocity)	10.6	10.6	13.2	13.2

[a] The flow resistance term is based on interstitial velocity.
[b] The *A*, *B* and *C* terms used here are apparent van Deemter fit coefficients and thus are different from the values obtained from theoretical modeling such as those reported by Gritti et al.
[c] The *B* terms are typical values for a compound with k' about 5.

true. In addition, the optimal particle size or column length might not be commercially available. Compromises need to be made in such cases [30]. Nevertheless, conducting a full three-parameter optimization can provide important insights into the *performance potential* of a given type of particle. Thus we first use this approach to compare the four different types of particles. As the particle size is varied, in this section, we use 600 bar SPPs, 1000 bar SPPs, 1000 bar totally porous and 600 bar traditional totally porous to refer to sub-3-μm SPPs, sub-2-μm SPPs, sub-2-μm totally porous particles and traditional totally porous particles, respectively.

In the three-parameter optimization, the optimal particle size, column length and linear velocity are calculated via Eqs. (1)–(3). Interested readers are referred to Ref. [24] for details of these equations.

$$d_p^* = \left[\frac{\phi\eta B}{P_{max}C}\right]^{1/4} (\lambda t_o)^{1/4} D_m^{1/2} \quad (1)$$

$$L^* = \left[\frac{P_{max}B}{\phi\eta C}\right]^{1/4} (\lambda t_o)^{3/4} D_m^{1/2} \quad (2)$$

$$u_e^* = \left[\frac{P_{max}B}{\phi\eta C}\right]^{1/4} (\lambda t_o)^{-1/4} D_m^{1/2} \quad (3)$$

where ϕ is the flow resistance, η is the mobile phase viscosity, P_{max} is the maximum operating pressure, λ is the ratio of interstitial porosity and total porosity, D_m is the solute diffusion coefficient in the mobile phase, and t_0 is the column dead time. Clearly as time decreases, one needs to use smaller particles with shorter columns at higher linear velocity. For SPPs, we assume the ratio ρ is kept constant as particle size is varied. If the exact particle size, column length and velocity calculated from Eqs. (1)–(3) are available, one can achieve the highest possible plates, as shown in Eq. (4):

$$N_{max} = \left[\frac{P_{max}\lambda t_o}{\phi\eta}\right]^{1/2} \frac{1}{h_{min}} \quad (4)$$

Eq. (4) is very informative. There are three terms that vary significantly between different particles: maximum operating pressure, λ the ratio of interstitial and total porosity, and minimum HETP. Plugging the values in Table 1 into Eq. (4) immediately gives the following order of N_{max}: 600 bar SPPs > 1000 bar SPPs > 1000 bar totally porous > 600 bar traditional totally porous. This comparison can also be presented graphically using speed (t_0/N) vs. efficiency (N) as shown in Fig. 2. Each line is the ultimate performance limit of every particle type at its maximum pressure, which is often called the 'Knox–Saleem line' [6,31]. Different points on each line correspond to different combinations of particle size, column length and linear velocity as given by Eqs. (1)–(3). It is evident that the 600 bar SPPs always provide the best performance in the whole analysis time range in Fig. 2. This is mainly due to its 30% or lower h_{min} compared to the other particle types, despite its lower maximum pressure (due to the square root dependence of pressure in Eq. (4)). This clearly highlights the *performance potential* of such SPPs, assuming the impressive h_{min} can be achieved for any particle size in any column dimension (including diameter).

Table 2 lists the optimum particle size, column length and linear velocity for each particle type at three different analysis times. In Fig. 2, the points where the optimal particle sizes are 1.8, 2.7, 3.5 and 5 μm are labeled as diamonds, squares, circles and triangles on each line, respectively. Interestingly ultrafast separations with t_0 < 10 s require optimal particle sizes smaller than 1.8 μm for all four particle types. Therefore, the use of 1.8 μm particles for these applications represents a deviation from the three-parameter optimum, resulting in efficiency less than optimum [30]. On the other hand, ultrahigh efficiency separations with t_0 > 1000 s require particle sizes larger than 5 μm for all four particle types.

2.2.2. Two-parameter optimization

Compared to the three-parameter optimization, particle size is fixed in the two-parameter optimization and only column length and flow rate are varied to achieve the highest efficiency in a given time [24–26]. Therefore, we fix the particle size to 2.7 μm, 1.7 μm, 1.8 μm and 3.0 μm for sub-3-μm SPPs, sub-2-μm SPPs, sub-2-μm totally porous and traditional totally porous particles, respectively. They represent the commonly used sizes for each particle type. If

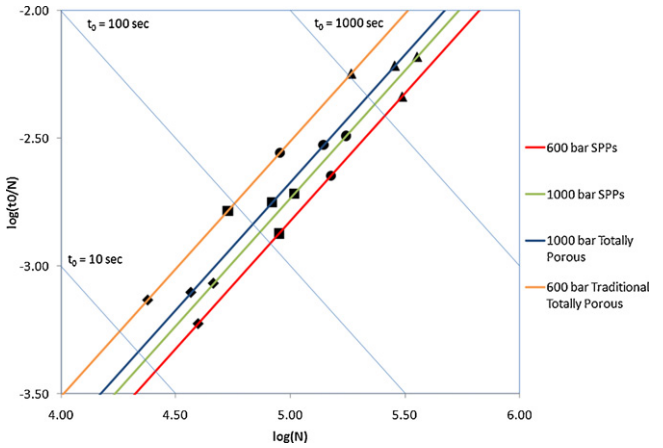

Fig. 2. The three-parameter optimum lines for four different types of particles. Calculation conditions: 40 °C, 30/70 acetonitrile/water, D_m is 1.0×10^{-5} cm^2/s. The diamonds, squares, circles and triangles represent the points on each line where the optimal particle size is 1.8, 2.7, 3.5 and 5.0 μm, respectively.

Table 2
Three-parameter optimization results for four types of particles at different analysis time.

Particle type	600 bar SPPs	1000 bar SPPs	1000 bar totally porous	600 bar traditional totally porous
Typical particle size	Sub-3-μm	Sub-2-μm	Sub-2-μm	2.5-5.0 μm
t_0 = 10 s (t_R = 1 min)				
Optimum d_p (μm)	1.5	1.3	1.4	1.6
Optimum L (cm)	5.6	6.4	6.4	5.7
Optimum u_e (cm/s)	0.73	0.83	0.96	0.84
N_{max}	25,900	23,300	21,700	18,000
t_0 = 100 s (t_R = 10 min)				
Optimum d_p (μm)	2.6	2.3	2.5	2.8
Optimum L (cm)	32	36	36	32
Optimum u_e (cm/s)	0.41	0.47	0.54	0.47
N_{max}	81,800	73,600	68,500	57,000
t_0 = 1000 s (t_R = 100 min)				
Optimum d_p (μm)	4.6	4.0	4.4	5.0
Optimum L (cm)	178	202	204	179
Optimum u_e (cm/s)	0.23	0.26	0.30	0.27
N_{max}	258,600	230,800	216,500	180,300

[a]Calculation conditions: 40 °C, 30/70 acetonitrile/water, D_m is 1.0×10^{-5} cm^2/s.

the chosen particle size is close to the size predicted in the three-parameter optimization, one will achieve excellent separations. Otherwise the loss of efficiency at the two-parameter optimum vs. three-parameter optimum might be substantial [30].

The optimal column length and linear velocity in the two-parameter case are given by:

$$L^* = \left[\frac{P_{max}\lambda t_o}{\phi\eta}\right]^{1/2} d_p \quad (5)$$

$$u_e^* = \left[\frac{P_{max}}{\phi\eta\lambda t_o}\right]^{1/2} d_p \quad (6)$$

where d_p is the fixed particle size. It is important to note that the combination of column length and linear velocity in Eqs. (5) and (6) always generate the maximum pressure. When the results of the two-parameter optimization are presented in a "Poppe plot", two asymptotes become obvious: the vertical asymptote that represents the limiting efficiency (N) and the horizontal asymptote that represents the limiting speed (t_0/N), see Fig. 3. They are given by:

$$N_{lim} = \frac{P_{max} d_p^2}{\phi\eta B D_m} \quad (7)$$

$$\left(\frac{t_0}{N}\right)_{lim} = \frac{C d_p^2}{\lambda D_m} \quad (8)$$

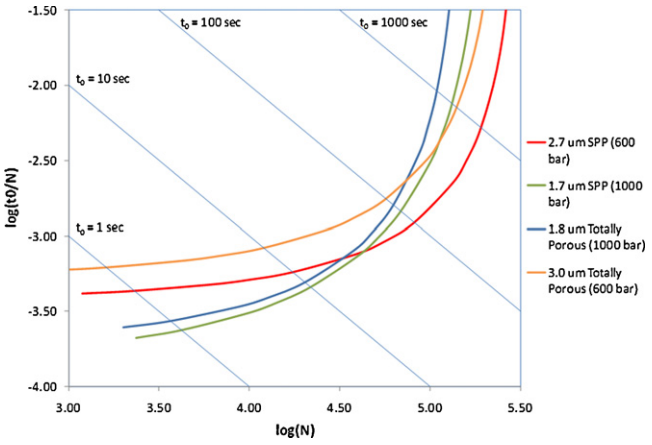

Fig. 3. The two-parameter optimum curves for four different particles. Calculation conditions: 40 °C, 30/70 acetonitrile/water, D_m is 1.0×10^{-5} cm^2/s.

Therefore, higher limiting efficiency would require higher maximum pressures, larger particle sizes and smaller van Deemter B terms. On the other hand, faster limiting speed would require smaller particle sizes and smaller van Deemter C terms.

The Poppe plots for the four particles are shown in Fig. 3. The optimum length, linear velocity and the resulting plates for short, intermediate and long analyses are also listed in Table 3. It is clear from Fig. 3 that both 1.7 μm SPPs and 1.8 μm totally porous particles are good for very fast separations. In fact, both of these particles outperform the 2.7 μm SPPs when the column dead time is shorter than 30 s (the crossover points). It is clear in Table 3 that 26% higher plates can be obtained for a t_0 = 10 s separation on the 1.7 μm SPPs at 1000 bar, compared to the 2.7 μm SPPs at 600 bar. On the other hand, the 2.7 μm SPPs start to outperform the sub-2-μm particles as the column dead time increases above t_0 of 30 s. For a typical separation at t_0 = 100 s, the 2.7 μm SPPs give 18% more plates than the 1.7 μm SPPs. As analysis time increases further at t_0 = 1000 s, almost twice as many plates can be achieved on the 2.7 μm SPPs compared to the 1.8 μm totally porous particles. This prediction has been confirmed theoretically and experimentally [19,23]. If the 2.7 μm SPPs could be operated at 1000 bar, even better results could be obtained especially at long analysis times [19,32]. Interestingly, the 3.0 μm totally porous particles never provide the best performance in the analysis time range in Fig. 3, primarily due to their larger B term and lower maximum operating pressure. However, if 5 μm totally porous particles were used in the calculation, they would be the best choice for conducting ultrahigh efficiency separations due to the square dependence of limiting efficiency on particle size (see Eq. (7)) [33].

It should be noted that the optimum column lengths when column dead time is longer than 100 s are longer than most commercially available columns (e.g. >25 cm, see Table 3). One would have to couple columns in series in order to fully realize the potential of the particles. This emphasizes an unfortunate reality, in that practitioners limit their method development to the commercially available column lengths. A direct consequence of this is that one might choose a column length that is far from the optimum, thus settling for suboptimal separations. If such a limitation is unavoidable, it would be better to perform a two-parameter optimization with practical constraints [34]. Alternatively, some automated column coupling systems have been developed to achieve different column lengths, especially during method development [35].

2.2.3. Summary

When we use the three-parameter optimization to assess the performance potential of different types of particles, we discover

Table 3
Two-parameter optimization results for four particles at different analysis time.

Optimization results	2.7 μm SPPs (600 bar)	1.7 μm SPPs (1000 bar)	1.8 μm totally porous (1000 bar)	3.0 μm totally porous (600 bar)
t_0 = 10 s (t_R = 1 min)				
Optimum L (cm)	10.5	8.5	8.4	10.9
Optimum u_e (cm/s)	1.36	1.11	1.25	1.63
N_{max}	17,300	21,800	20,200	11,900
t_0 = 100 s (t_R = 10 min)				
Optimum L (cm)	33	27	27	34
Optimum u_e (cm/s)	0.43	0.35	0.40	0.51
N_{max}	81,600	68,900	62,400	56,700
t_0 = 1000 s (t_R = 100 min)				
Optimum L (cm)	105	85	84	109
Optimum u_e (cm/s)	0.14	0.11	0.13	0.16
N_{max}	191,600	132,700	108,900	140,000

[a]Calculation conditions: 40 °C, 30/70 acetonitrile/water, D_m is 1.0×10^{-5} cm^2/s.

that the particle type with the properties of modern sub-3-μm SPPs (albeit at lower pressure of 600 bar) will always provide the best separation performance in *any* analysis time. This superior performance is mainly due to their substantially lower h_{min} and highlights the *potential* of SPPs. Clearly this is based on the assumption that key features responsible for the success of the SPPs can be reproduced on different particle sizes and different column dimensions.

When we conduct the more practically relevant two-parameter optimization to compare different currently available particles, we learn that:

1. The 2.7 μm SPPs give superior performance over the other three particles in a very wide analysis time range, i.e. when column dead time is longer than about 30 s (or t_R > 3 min). In addition, this advantage increases as analysis time increases.
2. For ultrafast separations, the sub-2-μm SPPs or totally porous particles provide better solutions. It is worth mentioning that the 2.7 μm SPPs can be run on a traditional HPLC at <600 bar, assuming the system extra-column broadening is minimized. Thus it can be a viable option to achieve ultrafast separations with slightly lower efficiency, but without a large investment in ultrahigh pressure instruments.
3. For a wide range of analysis times, the optimum column lengths for 2.7 μm SPPs are longer than the commercially available lengths that analysts are used to (e.g. 3–25 cm). This could lead to significant loss in efficiency when these longer column lengths are not used.

These are important conclusions as they highlight the performance potential of the modern SPPs and can direct future development of this area. In the next section, we show some successful applications that use SPPs and highlight the benefit of such materials.

3. Applications of modern superficially porous particles

Since the commercial introduction of HPLC columns containing modern, sub-3-μm SPPs in 2006, there have been many applications of these columns published in the peer-reviewed literature as well as conference proceedings and vendor application and technical notes. It is not our intention here to provide a comprehensive review of these applications but rather to select a few examples that illustrate the use of the various particle types over a wide range of applications, analysis times and sample types.

3.1. Small molecules applications

3.1.1. Ultrahigh speed

As shown in Fig. 1, many applications desire high speed and do not require high efficiency, due to relatively low sample complexity. Such applications include simple assay tests, cleaning validation, process monitoring and the second dimension of two-dimensional separations. Below we discuss some specific examples that utilize modern superficially porous particles.

The feasibility of using either sub-2-μm totally porous particles or 2.7 μm SPPs in an ultrafast HPLC method for dissolution testing has been demonstrated by Wang et al. [30]. In contrast to the use of representative column characteristics in the theoretical optimizations in Tables 1–3 above, they measured the actual column characteristics for a 1.8 μm ZORBAX RRHD SB-C18 column and a 2.7 μm Poroshell 120 SB-C18 column. They then applied three- and two-parameter optimization to find the optimal column length and flow rate that give the highest efficiency in the desired analysis time (column dead time of 4 s). They found that a 75 mm length was closest to the optimum for both columns at 80 °C, when the 1.8 μm ZORBAX RRHD and the 2.7 μm Poroshell 120 were operated at 1100 bar and 550 bar, respectively. Under these ultrahigh speed conditions, the 1.8 μm ZORBAX RRHD column exhibits the expected advantage over the 2.7 μm Poroshell 120 column for the methylparaben sample as predicted by Fig. 3. However, the 2.7 μm Poroshell 120 column separation required lower pressure and generated only slightly lower plates per second (i.e. 2000 vs. 2500, see Fig. 4). These ultrafast separations were applied in the dissolution test of ciprofloxacin extended release tablets and both columns were found to produce equivalent dissolution profiles to a conventional UV analysis, but within similar analysis time. The ability of HPLC to handle a wide sample concentration range combined with the demonstrated high speed analysis suggests that ultrafast LC would be ideal for simple assays such as dissolution and content uniformity tests.

Bioanalytical testing by LC–MS in pharmacokinetic studies is one application area that has quickly adopted the SPP technology, where high sample throughput is desired. This is because sub-3-μm SPPs offer similar peak capacities to those of sub-2-μm totally porous particles but at lower backpressure. In addition, the use of a larger column inlet frit for sub-3-μm SPPs presents less risk of column clogging when analyzing new drug candidates in biological matrices. The increasing popularity of SPPs is evident from the many published papers on this subject [36–40]. For example, Cunliffe et al. used a 2.1 mm × 50 mm column packed with 2.7 μm Ascentis Express particles to conduct fast gradient separations of Posaconazole in human plasma. The new method had a cycle time of about 1 min and was 4 times faster than an existing assay. The

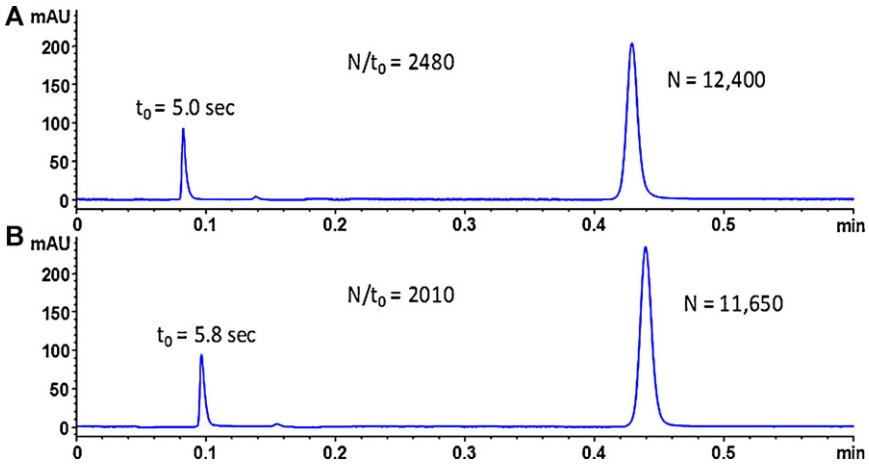

Fig. 4. Ultrafast analysis of methylparaben. LC conditions: mobile phase A is 0.1% TFA in water, mobile phase B is acetonitrile, 80 °C, 0.3 μL injection, 278 nm. Dead time marker was Uracil. (A) 1.8 μm ZORBAX RRHD SB-C18, 75 mm × 2.1 mm, 17% B, 2.00 mL/min, 1100 bar. (B) 2.7 μm Poroshell 120 SB-C18, 75 mm × 2.1 mm, 15% B, 1.81 mL/min, 550 bar.
From Ref. [30] with permission.

method was found to be very robust and can be routinely used for >1000 injections of clinical samples [37].

Another example of high-throughput analysis is shown by Alelyunas et al. [41], where they developed fast separations using SPPs for log*D* lipophilicity measurement. A high-speed analysis (≤3.2 min run time, $t_0 \approx 10$ s) was required that could complete two 96-well plates in an overnight run using an Agilent 1200 HPLC (600 bar pressure limit). Although this separation has a $t_0 \approx 10$ s, it also has a cycle time of about 3.2 min. Therefore, Fig. 3 and Table 3 suggest that the choice of optimum column could be either a sub-2-μm column (either totally porous or SPP with a 1000 bar pressure limit) or a 2.7 μm SPP column with a 600 bar pressure limit. In this case, a 2.7 μm, 2.1 mm × 30 mm C18 SPP column (Halo or Ascentis Express) was chosen as the best alternative due to the lower operating pressure but similar efficiency compared to the sub-2-μm columns.

Comprehensive, online two-dimensional liquid chromatography (2DLC) requires ultrahigh speed separations in the second dimensions to minimize the loss of peak capacity due to undersampling of the first dimension separation [42,43]. 2DLC has the potential for being particularly effective at separating closely related compounds provided that suitably orthogonal separation modes are chosen for the first and second dimensions. Stoll and co-workers used a 2.1 mm × 30 mm column packed with 2.7 μm Ascentis Express particles and achieved a 15 s separation of phenytoin that had a column dead time about 2 s, an efficiency about 4000 plates and a pressure about 300 bar [44]. This ultrafast separation was applied as the second dimension of a selective 2DLC system and enabled them to analyze as many as six fractions from a 6 s wide first dimension peak with a multi-loop storage system design. Carr et al. used the same dimension column but packed with 2.7 μm Halo C18 particles and achieved ultrafast gradient separation of peptides in less than 10 s [45]. Such ultrafast gradient should be powerful in generating fast comprehensive online 2DLC with high peak capacities. Alexander and Ma [46] demonstrated an RPLCxRPLC separation of an active pharmaceutical ingredient from an oxidative product and photo degradant. In the second dimension, they used two columns operated in parallel with a cycle time of 30 s for each gradient separation. Although Fig. 3 would predict that a column with a sub-2-μm media (either totally porous or SPP with a 1000 bar pressure limit) would be the preferred column choice, a 2.7 μm, 3.0 × 50 mm C18 SPP column (Ascentis Express) was chosen as the best alternative due to the pressure limitations of the second dimension pump hardware. Fig. 5 shows the consecutive chromatograms in one of the parallel second dimension separations. This 2DLC system allowed them to resolve impurities at very low level of 0.05% w/w, which would otherwise coelute with the main peak in the first dimension.

3.1.2. Speed and resolution

As the sample mixture or the sample matrix becomes more complex, longer columns with higher efficiencies, but consequently necessitating longer t_0 and analysis times, are required. These types of samples can include environmental, food, natural product or pharmaceutical samples containing impurities. Impurities are often present at low levels compared to the principal analytes and, in many cases, must be detected and quantified if present at the 0.05% level or higher.

Yang et al. [47] compared a 2.7 μm C18 SPP column (Ascentis Express) with 3.0 μm and 1.7 μm C18 totally porous particle columns (Atlantis T3 and Acquity BEH, respectively) for the analysis of a complex mixture of an agricultural product, derived from

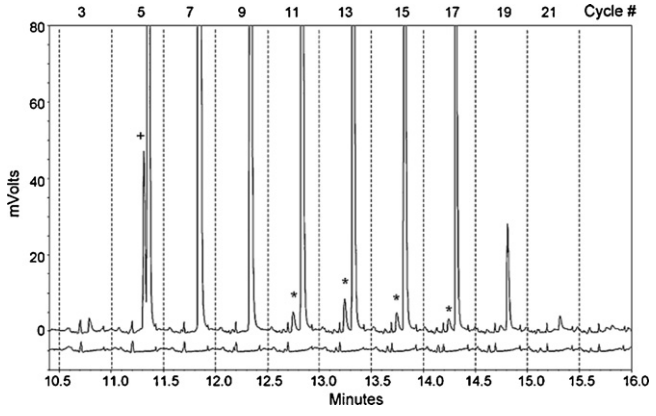

Fig. 5. RPLC × RPLC separation of a three component drug degradation mixture (API at 0.5 mg/mL, an oxidation product of the API at 1% (w/w), and a photo degradant of the API at 0.5%, w/w). Repetitive 30 s gradient separations on column A as recorded at 280 nm by Detector A. The lower trace shows the detector response from the solvent blank. The dotted lines every 15 s show the time-points at which the sampling valve switches. The peaks marked with a+ are from component 1 and those marked with a* are from component 2. The off-scale peaks are from the API.
From Ref. [46] with permission.

natural sources and containing up to 15 components including the principal analyte, various impurities and potentially residual proteins and surfactants. The columns were evaluated for separation efficiency, speed of analysis, backpressure, column lot-to-lot variability and long-term stability. These 15 components are all related structurally (similar molecular weights (600–700 Da), functional groups and polarities) and, therefore, require a higher resolution (longer) column to effectively separate them, particularly since an additional goal of this research was to achieve a suitable separation using isocratic conditions. 100 mm long columns were chosen for the 2.7 μm Ascentis Express and 1.7 μm Acquity BEH columns whereas a 150 mm long column was required for the 3.0 μm Atlantis T3 column. Both the 2.7 μm SPP and 1.7 μm totally porous particle columns provided acceptable separations in about one third of the time for the 3.0 μm Atlantis T3 column. The 1.7 μm BEH column gave about 35% more plates than the 2.7 μm SPP column primarily because the same column length was used. However, the 2.7 μm SPP column was preferred because the backpressure of the 1.7 μm BEH was at the pressure limit of the conventional HPLC instrument under the conditions used ($t_0 \approx 30$ s). If they were operated at the two-parameter optimum, a longer column would be needed for the 2.7 μm SPPs and similar plates would be obtained (see Table 3).

Screening methods using a range of fast to moderately fast gradient conditions can be used by the pharmaceutical industry to screen for impurities in APIs and for cleaning validation samples. Fekete et al. [48] compared the peak capacities and peak capacity per unit time per unit pressure of three commercially available 2.6–2.7 μm SPP C18 columns (Kinetex, Ascentis Express and Poroshell 120) to a 1.7 μm totally porous particle C18 column (BEH), in the separation of 14 polar APIs. They chose a linear gradient of 40–90% acetonitrile for all analyses but varied the gradient steepness by varying the gradient times (3–21 min) and flow rate (0.8–0.4 mL/min). Although there were performance differences between the three SPP columns, the peak capacities of the 2.7 μm SPP columns were similar or higher than the 1.7 μm totally porous particle column under most gradient conditions, which is consistent with the predictions of Table 3 (see Fig. 6). The peak capacity per unit time per unit pressure of the 2.7 μm SPP columns always exceeds that of the 1.7 μm totally porous column (see Fig. 7). A similar observation was also made by Abrahim et al. in a study of comparing 2.7 μm SPP to sub-2-μm totally porous particles for the application of impurity profiling in drug substances [49].

3.1.3. Ultrahigh resolution

Fig. 3 indicates that, once the t_0 of the separation exceeds about 30 s, the efficiency for 2.7 μm SPP columns will always be higher than totally porous particle columns of any particle diameter or even the 1.7 μm SPP column. Ultra-high resolution separations (>100,000 plates) should be achievable by connecting several columns in series. Such separations would be very useful for highly complex samples.

Gratzfeld-Hüsgen and Naegele [50] connected three 2.7 μm, 4.6 mm × 150 mm Poroshell 120 SB-C18 columns in series (45 cm total) and achieved ≈115,000 plates for a QC test mix in less than 4 min with a backpressure of 573 bar (see Fig. 8, $t_0 \approx 133$ s). Fig. 3 predicts that a t_0 of 133 s for the 2.7 μm SPP column should produce an optimum efficiency of 117,000 plates with a 47 cm column at 600 bar and their experimental result at 573 bar matches this prediction very well.

Cabooter et al. [23] also achieved >100,000 plates for a mixture of four pharmaceutical analytes by connecting four 2.7 μm, 2.1 mm × 150 mm Halo C18 columns in series (60 cm total) and evaluating the performance at 30, 50 and 80 °C. Flow rates were adjusted at each temperature to operate the column near the van Deemter optimum resulting in column pressures of 621, 577 and 510 bar for 30, 50 and 80 °C, respectively. Plate counts for the three most retained peaks exceeded 100,000 at all three temperatures and over a range of k' from 3 to 12.

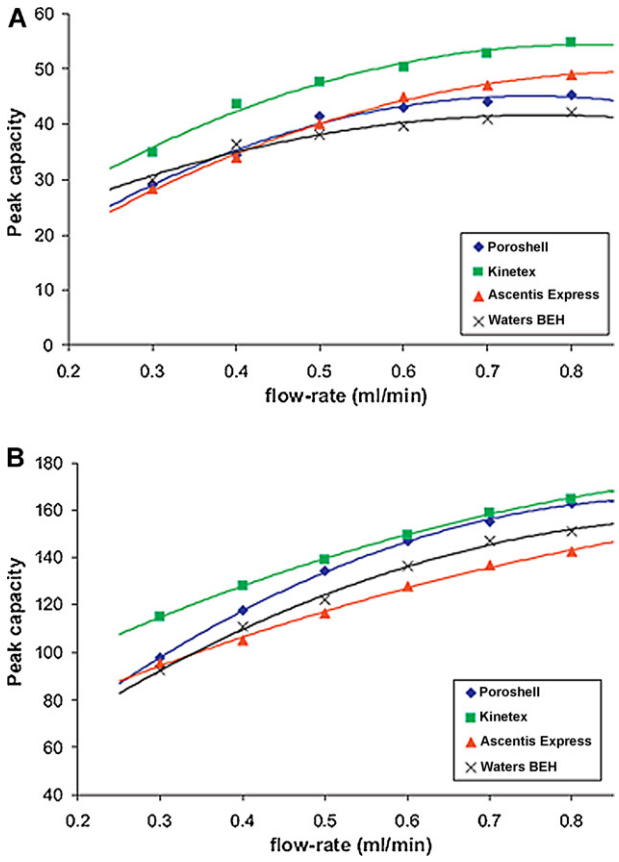

Fig. 6. Peak capacity plots as function of flow rate at (A) 3 min gradient time and (B) 21 min gradient time. Separation of 14 polar APIs, 2.1 mm × 50 mm columns, 2.6–2.7 μm SPP C18 (Kinetex, Ascentis Express and Poroshell 120) and a 1.7 μm totally porous particle C18 (BEH), linear gradient from 40% to 90% acetonitrile, 30 °C, 0.5 μL injection.
From Ref. [48] with permission.

Ultrahigh efficiency on coupled columns can also be achieved in HILIC mode as shown by McCalley [51]. He coupled three 2.7 μm, 4.6 mm × 150 mm Halo silica columns in series (45 cm total) and achieved between 100,000 and 107,000 plates for an isocratic HILIC separation of a mixture of acids and bases with an eluent of 85:15 acetontrile:0.1 M, pH 3.0 ammonium formate (1 mL/min) at 30 °C. The value for the plates achieved is expected for the 2.7 μm SPP column with a $t_0 \approx 193$ s (Fig. 3). In fact due to low mobile phase viscosities in HILIC mode, even higher efficiency would be possible by using much longer columns.

3.2. Large molecules applications

The recent resurgence and popularity of SPP columns has been due primarily to the development, commercialization and application of 1.7–2.7 μm SPPs with 90–120 Å pores to small molecule applications as discussed above. However, SPPs were first developed in the late 1960s by Horvath et al. [1,53] and Kirkland [52,54,55]. Kirkland applied these SPPs to the separations of large molecules such as proteins to take advantage of the improved mass transfer characteristics for these slow-diffusing molecules. In fact, the design intent of the second generation of commercial SPP columns (5 μm, 300 Å Poroshell) was also to provide a high resolution separation of macromolecules [56].

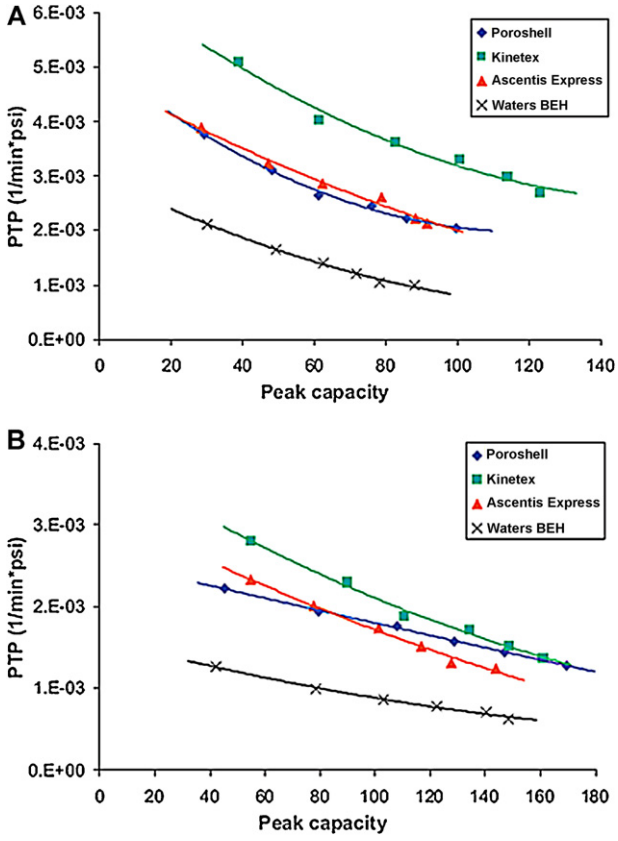

Fig. 7. Peak capacity per unit time per unit pressure at the flow rate of (A) 0.3 mL/min and (B) 0.8 mL/min. Separation of 14 polar APIs, 2.1 mm × 50 mm columns, 2.6–2.7 μm SPP C18 (Kinetex, Ascentis Express and Poroshell 120) and a 1.7 μm totally porous particle C18 (BEH), linear gradient from 40% to 90% acetonitrile, 30 °C, 0.5 μL injection.
From Ref. [48] with permission.

Indeed, higher efficiency separations are observed for proteins [57,58] and peptides [18] on 5 μm, 300 Å Poroshell SB-C18 columns compared to totally porous 5 μm, 300 Å ZORBAX SB-18, particularly at higher flow rates. Wang et al. [59] compared a 5 μm Poroshell 300SB-C8 (2.1 mm × 75 mm) to a totally porous, 5 μm ZORBAX 300SB-C8 (2.1 mm × 150 mm) for the separation of the disulfide isomers of four different human IgG2 antibodies. Even though the totally porous ZORBAX 300SB-C8 column was twice the length of the Poroshell 300SB-C8 column, the former could not resolve the disulfide isomers but the latter could resolve the IgG2 antibody into multiple peaks corresponding to different disulfide isomers. Ricker et al. [58] also showed the effect of phase chemistry on the separation selectivity of a mixture of IgG1 and IgG4 monoclonal antibodies.

Fig. 3 indicates that in the two-parameter optimization case, where flow rate and column length are varied but particle size is

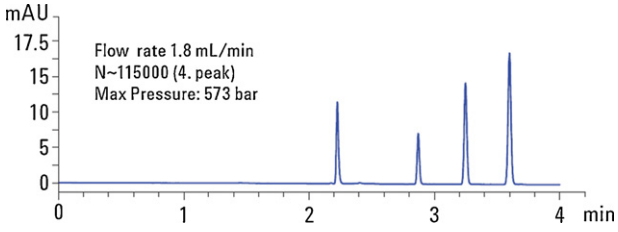

Fig. 8. Separation of thiourea, acetophenone, benzene and toluene on three coupled Poroshell 120 SB-C18, 4.6 mm × 150 mm, 2.7 μm columns. 20/80 water/acetonitrile, 1.8 mL/min, 60 °C, 254 nm.

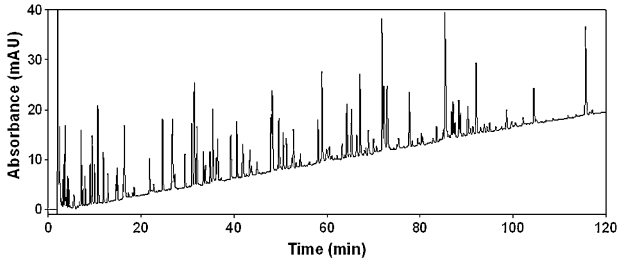

Fig. 9. Separation of BSA tryptic peptides on a 60 cm × 2.1 mm i.d. column set packed with 5 μm Poroshell 300SB-C18 particles. Mobile phase A: 0.1% TFA in water, mobile phase B: 0.1% TFA in 80/20 acetonitrile/water, gradient from 0% to 40% solvent B in 120 min, 0.50 mL/min, 70 °C.
From Ref. [18] with permission.

held constant and the column is operated at its maximum pressure, maximum resolution can be obtained at long times by using larger particle sizes and long columns [60]. This is not only true for small molecules with narrow pore columns but can also be applied to biomolecules with wide pore, SPP columns. For example, Wang et al. [18] did a gradient separation of a BSA tryptic digest on four Poroshell 300SB-C18 columns connected in series for a total length of 60 cm. They were able to achieve a peak capacity of >500 in 2 h (see Fig. 9).

Recent development and commercialization of the latest generation of SPP columns have not included media with pore sizes of 300 Å, which are required for macromolecule separations. However, a 160 Å SPP column was recently introduced by AMT and Sigma–Aldrich under the brand names of Halo Peptide ES-C18 and Ascentis Express Peptide ES-C18, respectively. Schuster et al. [13] compared the efficiency performance of the 160 Å Halo Peptide ES-C18 column to the original 90 Å Halo-C18 column for mixtures of peptides and small proteins. They found that the smaller peptides showed equivalent efficiency on both columns. However, the small proteins in the mixtures (i.e. ribonuclease, insulin, cytochrome *C* and lysozyme) showed broadened peaks on the 90 Å Halo-C18 column, indicating restricted diffusion, but narrow peaks on the 160 Å Halo Peptide ES-C18 column, indicating un-restricted diffusion (see Fig. 10). Gritti and Guiochon [14] studied the mass transfer kinetics of large molecules on the new Halo Peptide ES-C18 column and stated that the van Deemter *C* term for large molecules is mostly accounted for by a slow external film mass transfer. They concluded that the improved efficiency of the new Halo column for peptides and small proteins is related to the easier access and diffusion in and out of the larger pores. Since the 160 Å Halo Peptide ES-C18 was only recently introduced, more applications on large molecule separations are expected to be reported in the near future.

4. Practical aspects of the use of superficially porous particles

4.1. Instrument considerations

As more efficient columns are developed, better performing instruments are needed. For example, one should not expect good performance if a 2.1 mm × 50 mm column packed with 2.7 μm SPPs is used on a traditional HPLC without system dispersion optimization. Even with state-of-the-art UHPLC instruments, significant efficiency loss can occur for short narrow-bore columns packed with SPPs or sub-2-μm totally porous particles, especially for poorly retained compounds as clearly shown by many studies [29,61–63].

There are several sources of extra-column broadening, including finite injection volume, broadening in the injection system (e.g. valve, needle seat), broadening in connection tubing before and

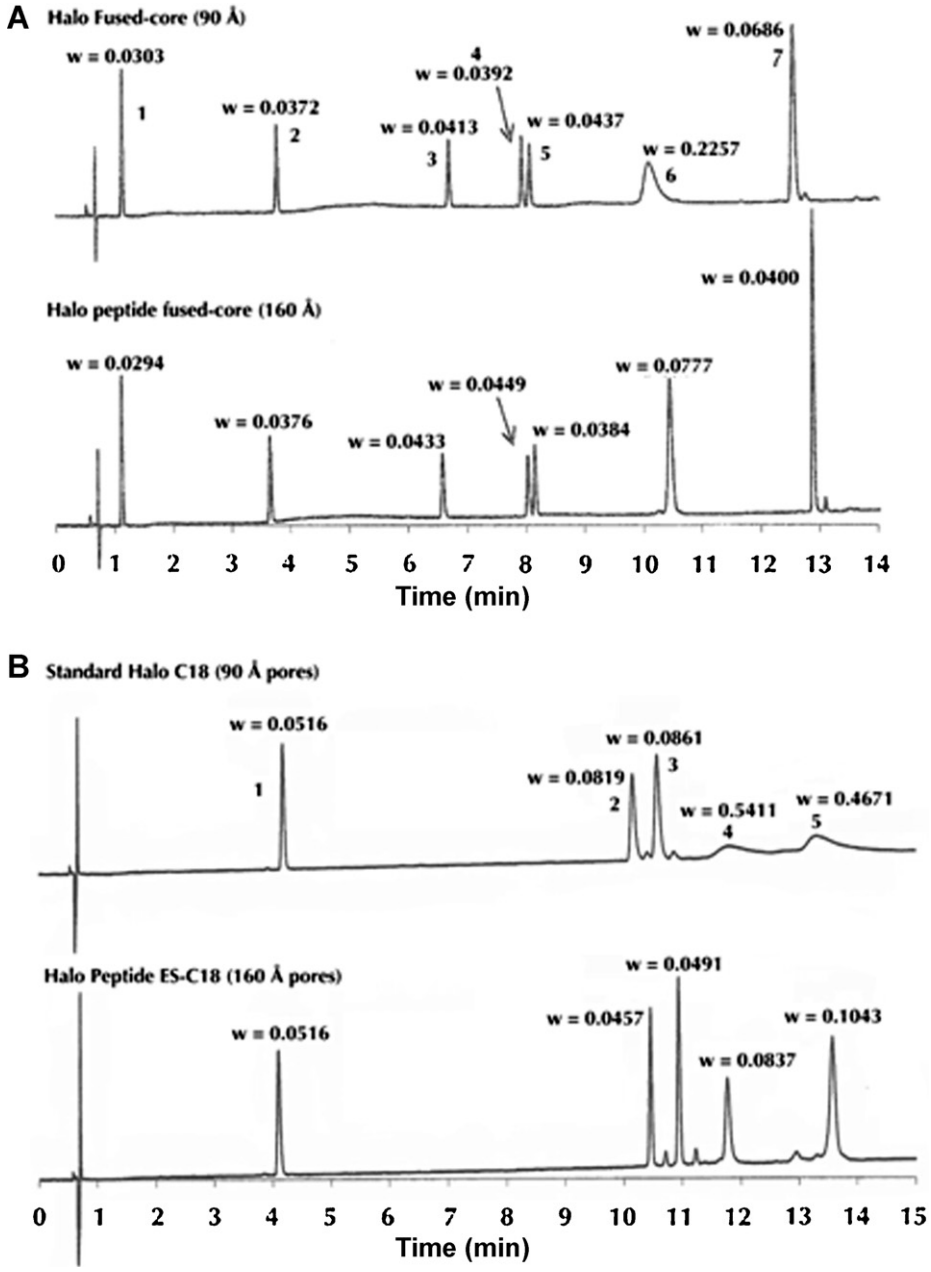

Fig. 10. Comparison of half-height peak widths for fused-core particles. Columns: 4.6 mm × 100 mm; 30 °C, 220 nm, water/acetonitrile gradient with 0.1% TFA. (Part A) Peptides, 1, Gly-Tyr; 2, Val-Tyr-Val; 3, Met Enkephalin; 4, Angiotensin II; 5, Leu-Enkephalin; 6, bovine ribonuclease; 7, insulin; gradient: 0% B to 50% B in 15 min; flow rate: 1.5 mL/min. (Part B) Peptides and small proteins, 1, Enk-Leu; 2, bovine insulin; 3, human insulin; 4, cytochrome *C*; 5, lysozyme; gradient: 15% B to 50% B in 15 min. From Ref. [13] with permission.

after the column, detector flow cell volume and finite detector time constant. We do not discuss these individual contributions here as a detailed discussion can be found in the paper by Gritti et al. [64]. Instead, we discuss the impact of extra-column broadening on the performance of highly efficient particles in the context of the comparison shown in Section 2.2.2.

A convenient way to characterize instrument dispersion is to measure the extra-column broadening in volumetric variance as shown by many authors [29,61–63,65]. The absolute value can vary significantly depending on the instrument model and LC conditions, such as analyte, mobile phase and temperature. Nevertheless a representative extra-column variance as a function of flow rate on a modern UHPLC instrument is given in Fig. 11. This curve is generated by Eq. (9), as used by Neue and co-workers [63], where F is the volumetric flow rate. The extra-column volume is assumed to be about 12 μL and the variance is about 6 μL^2 at 1 mL/min. The extra-column volume and variance can be applied to the three-parameter or two-parameter optimization results via Eq. (10) to assess the impact of the instrument on chromatographic performance, as shown by Desmet et al. [65]:

$$\sigma^2_{v,\mathrm{ex}} = \frac{19.4}{3 + 0.19/F}(\mu L^2) \tag{9}$$

$$N_{\mathrm{tot}} = \frac{V^2_{\mathrm{tot}}}{\sigma^2_{\mathrm{tot}}} = \frac{(V_m(1+k') + V_{\mathrm{ex}})^2}{(\sigma^2_{v,\mathrm{col}} + \sigma^2_{v,\mathrm{ex}})} \tag{10}$$

where V_m is the column dead volume, k' is the retention factor, V_{ex} is the extra-column volume, $\sigma^2_{v,\mathrm{col}}$ is the peak variance from the column and $\sigma^2_{v,\mathrm{ex}}$ is the extra-column peak variance.

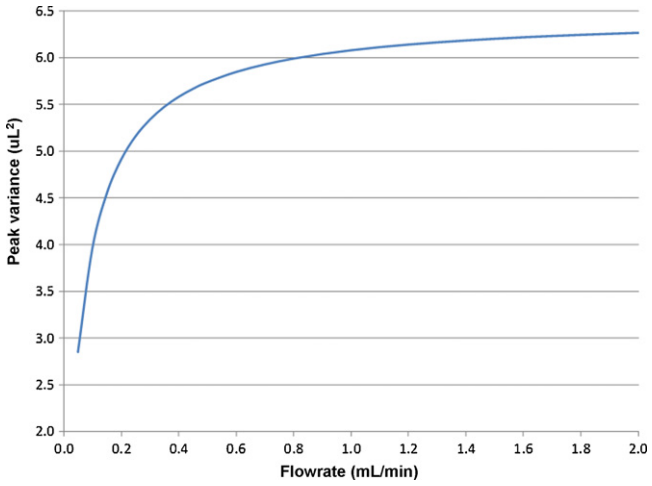

Fig. 11. Extra-column broadening as a function of flow rate on a typical UHPLC instrument. The extra-column volume is assumed to be 12 μL.

Eq. (10) suggests that the effect of extra-column broadening depends strongly on the solute retention factor k'. Fig. 12 shows the loss of plates of 2.7 μm SPPs at the two-parameter optimum on an instrument with extra-column broadening given in Fig. 11, for different retention factors at three analysis times. It is clear that the loss in plates increases as k' decreases and can be as big as 40% for a k' of 1. In addition, the loss in plates is more significant for fast separations, where short columns are operated at very high flow rate, generating very narrow peaks.

Not only does the extra-column broadening cause efficiency loss, but it also affects the relative performance of different particles. Fig. 13 shows the Poppe plots of 2.7 μm SPPs at 600 bar and 1.8 μm totally porous particles at 1000 bar, with and without extra-column broadening for a compound with k' about 2. An important observation is that the impact of extra-column broadening is different for different particles under two-parameter optimization. The efficiency loss for 2.7 μm SPPs is less than that for 1.8 μm totally porous particles. This is mainly due to the fact that the 1.8 μm totally porous particles require shorter columns at higher flow rate at the optimum conditions, thus generating narrower peaks compared to the 2.7 μm SPPs. For example, at a t_0 of 10 s, the optimum column length for 2.7 μm SPPs is 105 mm generating a peak with a variance of 18 μL^2. This is larger compared to the 12 μL^2 peak variance on the optimum 84 mm column for 1.8 μm totally porous particles, and is thus less susceptible to efficiency loss due to extra-column broadening. As a result, the crossover point of 2.7 μm SPPs and 1.8 μm totally porous particles decreases from 25 s to 14 s after applying extra-column broadening, and so the time range within which the 2.7 μm SPPs give superior performance increases. This is an important but underappreciated feature of sub-3-μm SPPs, possibly because many practitioners tend to use the same column length when changing from sub-2-μm totally porous to sub-3-μm SPPs thus deviating from the two-parameter optimum.

4.2. Sample mass loading capacity

Sample loading capacity at the analytical scale can be measured as the sample mass that causes a 50% efficiency loss compared to the efficiency when an infinitely small amount of sample is injected [66]. It is proportional to the total surface area per volume within a column. The specific surface area of SPPs from BET measurement in m^2/g is lower than that of totally porous particles due to the solid core. However, this is partially compensated by the higher density of SPPs [67].

In order to look at the impact of particle morphology, we compare two ideal particles with the same pore structure, one is totally porous and the other is SPP, as shown in Fig. 14. The intra-particle porosity and specific surface area of the totally porous particle and the shell layer of SPPs are described as ε_p and A_{sp}, respectively. The weight of porous silica (i.e. excluding the solid core) inside a column is given by Eq. (11), where V_{column} is the volume of the empty column tube, ρ is the ratio of the core diameter and the particle diameter, and D_{silica} is the density of the silica skeleton, approximately 2.2 g/cm^3:

$$W_{\text{porous silica}} = V_{\text{silica}} \cdot D_{\text{silica}} = V_{\text{column}} \cdot (1-\varepsilon_e) \cdot (1-\rho^3) \cdot (1-\varepsilon_p) \cdot D_{\text{silica}} \quad (11)$$

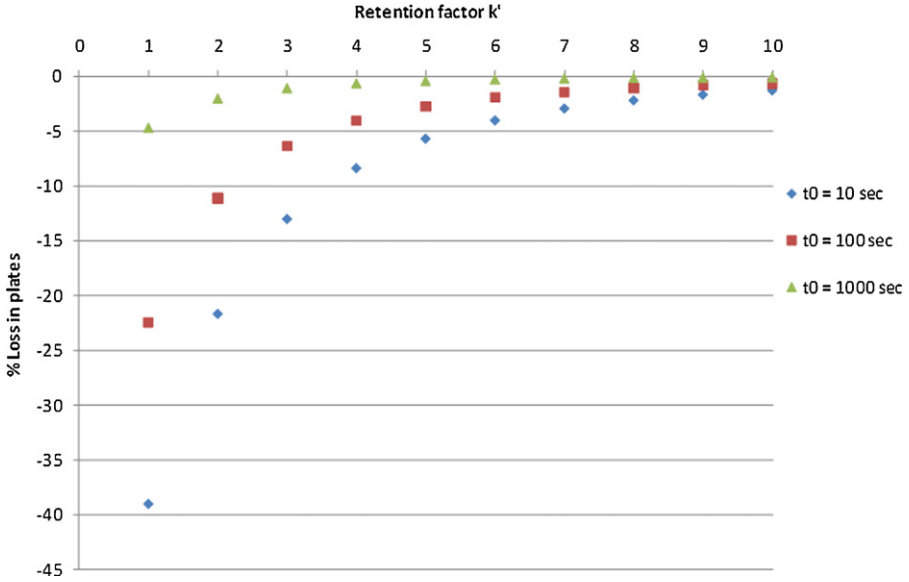

Fig. 12. Effect of extra-column broadening on efficiency loss as a function of solute retention for two-parameter optimum of 2.7 μm SPPs at 600 bar maximum pressure. Calculation conditions: 40 °C, 30/70 acetonitrile/water, D_m is 1.0×10^{-5} cm^2/s.

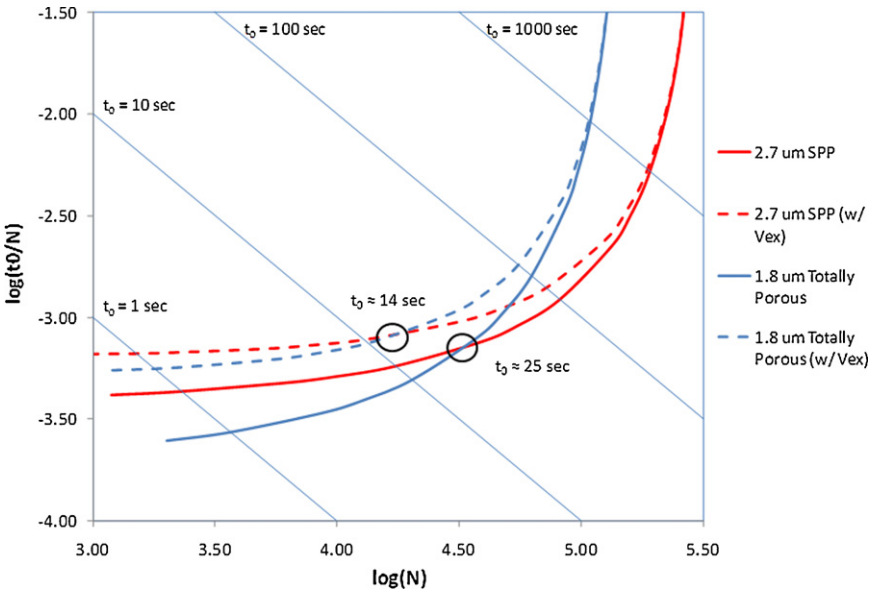

Fig. 13. The two-parameter optimum curves for 2.7 μm SPPs at 600 bar and 1.8 μm totally porous particles at 1000 bar. The solid curves exclude extra-column broadening and the dashed curves include extra-column broadening, assuming a k' of 2. Calculation conditions: 40 °C, 30/70 acetonitrile/water, D_m is 1.0×10^{-5} cm^2/s.

Therefore the total surface area per volume of the column is:

$$\frac{A_{\text{total}}}{V_{\text{column}}} = A_{sp} \cdot \frac{W_{\text{porous silica}}}{V_{\text{column}}}$$
$$= A_{\text{sp}} \cdot (1-\varepsilon_e) \cdot (1-\rho^3) \cdot (1-\varepsilon_p) \cdot D_{\text{silica}} \quad (12)$$

If we assume the same pore structure and similar interstitial porosity, the ratio of sample loading capacity between SPPs and totally porous particles is approximately the volume fraction of the shell layer $(1-\rho^3)$. If we assume a d_p of 2.7 μm and a d_c of 1.7 μm for the particles shown in Fig. 14, the ratio would be about 75%.

There have been several reports that study the sample loading capacity of SPPs [32,49,51,67,68]. In reality, sample loading capacity is affected by many factors in addition to total surface area per volume, including analyte properties, mobile phase conditions and surface chemistry of the particles. For example, a slight surface modification on the same base particle can substantially change the loading capacity of basic compounds [69]. Therefore it is difficult to conclude that the experimental difference is caused solely by the different particle morphology. Fig. 15 shows good examples where SPPs can have identical or even slightly higher loading capacity than totally porous particles. In this work, increasing analyte mass was injected on to the column and sample loading capacity was measured at 50% of the efficiency at the lowest sample loading. Clearly Poroshell 120 EC-C18 has the same loading capacity as Eclipse Plus C18 for neutral and acidic compounds. For basic compounds, Poroshell 120 column might have slightly higher loading capacity. This behavior is likely caused by the different pore structures and slightly different surface chemistry between these two particles.

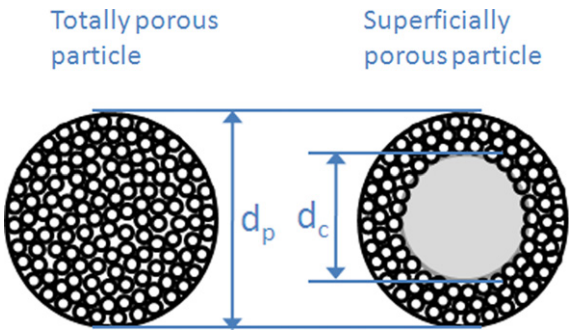

Fig. 14. Comparison of totally porous and superficially porous particles.

4.3. Method translation from totally porous particles to SPPs

General method translation was recently discussed by Majors [70]. In this section, we focus our discussion on the specific case of translating traditional HPLC methods with traditional totally porous particles to faster methods with sub-3-μm SPPs.

Chromatographers translate methods for different purposes. One might want to achieve higher resolution with the same analysis time, or to achieve a faster separation while maintaining resolution. The latter case is the most commonly encountered when one wants to improve productivity with an established method. This can be achieved by switching from larger totally porous particles to smaller totally porous particles, which is straightforward although an investment in UHPLC instrument is often required to fully utilize the sub-2-μm particles [71]. On the other hand, method translation from large totally porous particles to sub-3-μm SPPs can be more complex due to their different particle morphology and chromatographic behavior.

4.3.1. Isocratic methods

Isocratic resolution is affected by efficiency, selectivity and retention factor. Assuming the same phase chemistry is available on both totally porous and SPPs, the selectivity is approximately the same. A slightly weaker mobile phase can be used on the SPPs compared to the totally porous particles to compensate for the lower surface area in order to achieve the same k'. Therefore, the main challenge to translate the method with the same resolution is to achieve the same efficiency, i.e. plates.

We use the USP Naproxen Method as an example. The original method uses a 4.6 mm × 150 mm column packed with 5 μm totally porous particles and is about 10 min long. For the purpose of demonstration here, suppose the goal is to develop a faster method with the same resolution using the 2.7 μm SPPs. A quick approach for such translation is to use the common practice of keeping the same ratio of column length to particle

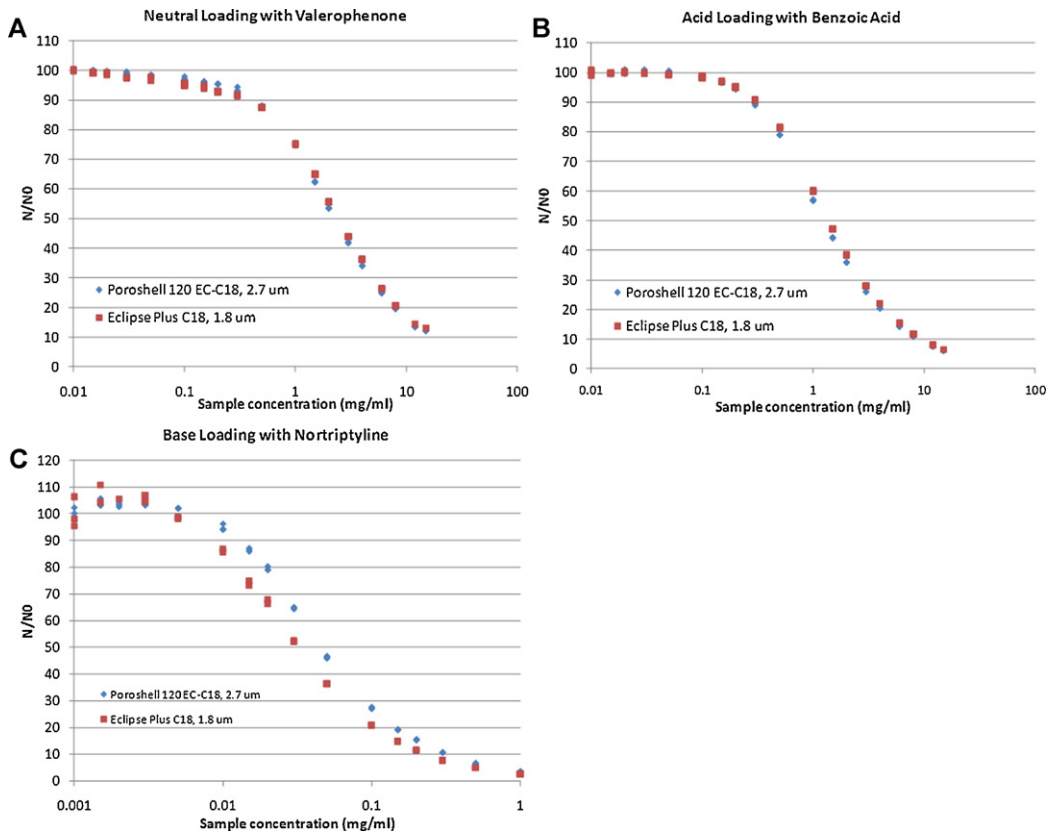

Fig. 15. Sample loading curves of totally porous particles and SPP particles: (a) neutral compound—valerophenone,,50 % ACN (b) acidic compound—benzoic acid, 15% ACN and (c) basic compound—Nortriptyline, 30 % ACN Columns were 3.0 mm x 100 mm, mobile phase A: 25 mM NaH2PO4 buffer pH 3.0, mobile phase B: acetonitrile, 30 °C.

size (see Eq. (13)). Therefore, we can use a 4.6 mm × 75 mm column packed with 2.7 μm SPPs. Although the SPP particle size is larger than half of the original particle size, one would probably expect more plates since SPPs give much improved reduced plate height. To operate at a similar reduced linear velocity, the flow rate is doubled on the 2.7 μm SPPs. Such translation results in the new method #1 in Table 4, which gives higher pressure, is more efficient and is much faster (4.4× faster) than the original.

$$N = \frac{L}{h \cdot d_p} \tag{13}$$

The pressure of the quick translation SPP method is 215 bar and is still lower than the pressure capability of the column and instrument. A further gain in separation speed can be achieved by conducting the two-parameter optimization discussed above to find the optimal column length and flow rate. In this case, we set the operating pressure to 500 bar to avoid running at the absolute maximum of the column. It should be noted that the use of 4.6 mm i.d. columns requires quite high flow rates at the optimum condition, which generate high backpressure from the instrument. Therefore, the available pressure on the column is significantly reduced. To account for this effect, instrument backpressure was measured as a function of flow rate and this is included in the calculation. The details of the calculation will be described in a future publication.

The new method #2 in Table 4 is the calculated two-parameter optimum for 2.7 μm SPPs. Calculation suggests the use of a 4.6 mm × 85 mm column at 3.7 mL/min. This method would give the same plates as the original method but is six times faster.

Table 4
Calculations of USP Naproxen method translation from traditional totally porous to sub-3-μm SPPs.[a]

Method	Original method	New method #1	New method #2[b]	New method #3[b]
Translation approach		Quick translation	Optimized translation	Practical optimum
Particle	5 μm totally porous	2.7 μm SPP	2.7 μm SPP	2.7 μm SPP
L (mm)	150	75	85	75
F (mL/min)	1.2	2.4	3.7	4.0
Pressure (bar)	66	215	500[c]	500[c]
N	14,700	17,500	15,000	14,200
t_0 (s)	71	16	12	10
N/t_0	208	1080	1250	1420
V_{inj} (μL)	20	10	11	10
Gain in speed[d]	–	4.4×	5.9×	7.1×

[a] Chromatographic conditions: mobile phase is 50/49/1 ACN/H_2O/acetic acid, room temperature, column i.d. is 4.6 mm.
[b] Two-parameter optimization was conducted at a maximum pressure of 500 bar at 25 °C, without extra-column broadening contribution.
[c] These are the total system pressure, including the column pressure and extra-column pressure. The extra-column pressure is assumed to be 35 × flow rate (bar).
[d] The gain in speed is the ratio of column dead time between the original method and the new method.

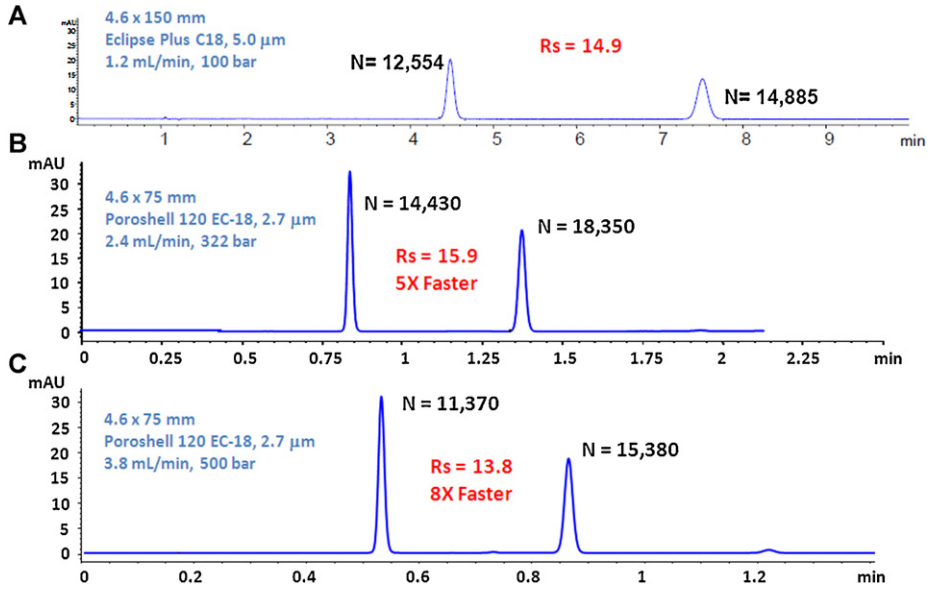

Fig. 16. Translating USP Naproxen method from 5 µm totally porous particles to 2.7 µm SPPs. Chromatographic conditions: 50:49:1 ACN:H_2O:acetic acid, peak 1 is Naproxen, peak 2 is Butyrophenone.

However, this is an ideal optimum and is not practically feasible as 85 mm columns are not commercially available. In such cases, a compromise needs to be made to use the closest commercially available column, i.e. 75 mm [30]. Such compromise results in a slight loss in plates due to the shorter column, but an even faster analysis at the same pressure of 500 bar. The column dead time is only 10 s and so the separation takes about 1 min with a k' of 5 (see new method #3 in Table 4).

The actual separations achieved with the original HPLC method, new method #1 and new method #3 are shown in Fig. 16. It is evident that the quick translation approach of new method #1 results in a higher efficiency, a slightly higher resolution and a 5× gain in speed. More importantly, a bigger gain in speed (i.e. 8×) can be achieved by using the theoretically guided optimization approach as shown by new method #3. This ensures the best results are obtained when translating traditional HPLC method to sub-3-µm SPPs.

4.3.2. Gradient methods

Gradient method translation from totally porous to SPPs is slightly more complex than isocratic method translation. In addition to maintaining column efficiency as discussed above, one needs to maintain selectivity, which is mostly affected by gradient steepness [72]. Gradient steepness is defined as

$$b = \frac{S \cdot \Delta c \cdot V_m}{t_G \cdot F} = \frac{S \cdot \Delta c \cdot (\pi R^2 L \varepsilon_t)}{t_G \cdot F} \quad (14)$$

where S is the sensitivity of solute retention to eluent strength, Δc is the change in eluent strength during the gradient, t_G is gradient time, F is the flow rate, V_m is the column dead volume, R is the column radius, L is the column length and ε_t is the column total porosity. The S values on totally porous and SPPs often differ but only slightly [19]. The initial and final mobile phase compositions can be slightly lower on SPPs due to their lower surface area but Δc changes only slightly. A new optimum column length and flow rate can be obtained via the process described in the previous isocratic translation section. Therefore the only other term that is significantly different and needs to be considered to reach the same gradient steepness is the particle total porosity. With this value, one can easily calculate the gradient time that is needed to maintain gradient steepness on the SPPs according to Eq. (15):

$$t_{G,2} = t_{G,1} \frac{F_1 \cdot L_2 \cdot \varepsilon_{t,2}}{F_2 \cdot L_1 \cdot \varepsilon_{t,1}} \quad (15)$$

where subscript 1 is for the totally porous particles and subscript 2 is for the SPPs. As an example, we can look at the gradient method translation from the 5 µm totally porous column (ε_t = 0.57) in the original method to the 2.7 µm SPP column (ε_t = 0.52) in the new method #3, as given in Table 4. If we assume an original gradient time of 30 min, Eq. (15) suggests a new gradient time of only 4.1 min to maintain the gradient steepness and this represents a more than 7-fold gain in speed.

For modern SPPs, the shell thickness relative to the particle diameters is high, thus the total porosity of SPP columns is only slightly lower than columns of totally porous particles (see Table 1). Therefore, assuming similar phase chemistry is available, the change in gradient selectivity is very small. Fig. 17 shows the excellent correlation of gradient retention time of 66 compounds (neutral, base and acid) on totally porous particles and SPPs. This suggests the almost identical gradient selectivity on these two different particles. However, some SPPs have much smaller particle porosity, as in the case of Poroshell 300 (only 0.25 µm shell on a 5 µm particle). In such cases, very different gradient selectivity can be observed. Fig. 18 shows a peptide separation on 5 µm totally porous particles and 5 µm SPPs. Two pairs of peptides coelute on this type of SPP while being completely resolved on the totally porous particles.

5. Future possibilities of superficially porous particles

The impressive chromatographic performance of modern SPPs has stimulated much research activity in this area in the past few years. Applications with such particles continue to be developed and used in many industries on both HPLC and UHPLC systems. It is easy to foresee that quality control or contract research laboratories will soon receive methods with SPP columns from R&D laboratories. On the other hand, there are three areas where improvements

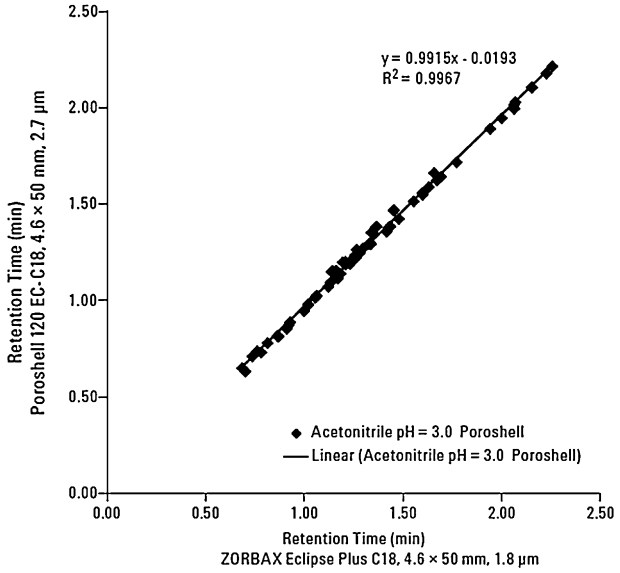

Fig. 17. Correlation of gradient retention times of 66 compounds on totally porous (ZORBAX Eclipse Plus C18) and SPPs (Poroshell 120 EC-C18). Mobile phase A: 10 mM ammonium formate pH 3.0, mobile phase B: acetonitrile, 2 mL/min, gradient from 5% B to 95% B in 2 min, 25 °C.

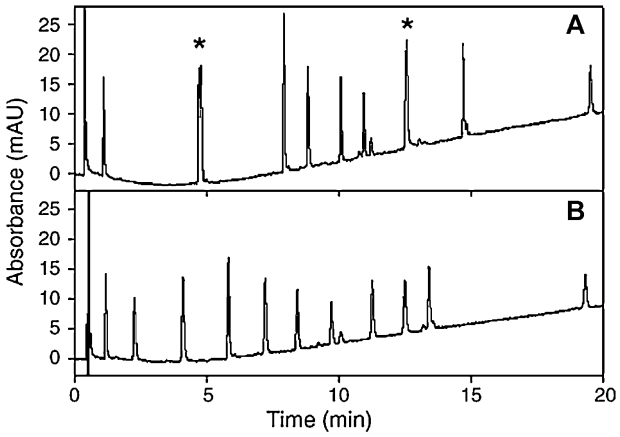

Fig. 18. Separation of the 11 test peptides in an acetonitrile/water gradient elution on (A) 5 μm Poroshell 300SB-C18 and (B) 5 μm ZORBAX 300SB-C18. The initial and final organic modifier fractions were adjusted on the two phases so that the first and last eluting peptides have approximately the same retention time. Asterisks in (A) indicate the co-elution of two peptides.
From Ref. [18] with permission.

might occur, including different SPP particle structure, more efficient column packing and more phase chemistries.

5.1. New particle structure

There are several possibilities for new particle structure.

• Different shell thickness.

The original premise of SPPs was to reduce the intra-particle diffusion distance of analytes. Thus it is natural to assume that a thinner shell leads to better efficiency, especially for larger molecules. Gritti et al. confirmed that the mass transfer resistance in SPPs is reduced by a factor of 2 compared to totally porous particles for small molecules [2]. However, its contribution to the better efficiency of SPPs is negligible compared to the effect of smaller eddy dispersion and longitudinal diffusion. Horvath et al. published a theoretical study on the effect of shell thickness on SPPs performance and suggested that a thinner shell should improve the separation efficiency, especially for large molecules [73]. Omamogho et al. made different SPPs with the same overall particle size (1.7 μm) but different shell thickness (150, 250 and 350 nm) and evaluated their chromatographic performance. They found that column efficiency increased in the order of decreasing shell thickness even for small molecules [74]. However, it is uncertain if such improvement in efficiency is directly caused by the thinner shell, or may be affected by the column packing process.

A major drawback of reducing shell thickness is the reduced porosity and thus the surface area, which strongly affects sample loading capacity and analyte retention. Therefore, the optimum shell thickness in reality is likely to be a compromise between efficiency and sample loading capacity, and is strongly sample dependent. It is unlikely that a single shell thickness will be the best for all applications. Guiochon et al. recently suggested that a better SPP should have a few shell layers of large porosity external to many shell layers of smaller porosity [75]. Such particles are yet to be made and evaluated to confirm the hypothesized chromatographic advantage.

• Different pore size.

Most of the recently introduced sub-3-μm and sub-2-μm SPPs have average pore size between 90 and 120 Å. While these pore sizes are adequate for small molecules, they are not ideal for larger molecules, as shown in several reports [13,14]. This observation certainly motivated the development of a wider pore material for peptide separation, such as the Halo Peptide-ES-C18 particles with an average pore size of 160 Å. This trend will likely continue and SPPs with even larger pores will likely be introduced for protein separations.

• Smaller particle size.

The most popular modern SPPs are about 2.6–2.7 μm in size but sub-2-μm SPPs are already commercially available. Jorgenson et al. recently reported studies on making 1.2 μm SPPs and their chromatographic behavior [76]. As in the case of totally porous particles, smaller SPPs would give higher efficiency but at the cost of dramatically increased pressure. In addition, packing sub-2-μm SPPs seems as challenging as packing sub-2-μm totally porous particles. Finally the reduction in absolute diffusion distance between SPPs and totally porous particles decreases as particles become smaller and this causes the benefit of smaller mass transfer resistance to disappear quickly. Therefore the success of making sub-2-μm or even sub-1-μm SPPs with similarly impressive chromatographic performance as sub-3-μm SPPs remains to be seen in the near future.

5.2. Better column packing of narrow bore columns

It is well known that narrow-bore columns (e.g. 2.1 mm i.d.) are more difficult to pack than normal-bore columns (e.g. 4.6 mm i.d.). For traditional totally porous particles, a well packed 4.6 mm i.d. column has an h_{min} of about 2 while a 2.1 mm i.d. column can have an h_{min} larger than 2.5. This problem is not so noticeable for sub-2-μm totally porous particles since column vendors typically make only narrow-bore columns for these small particles. On the other hand, this problem becomes obvious for modern SPPs since the remarkably low h_{min} of 1.5 can only be achieved on the 4.6 mm i.d. columns [2]. The h_{min} for 2.1 mm i.d. columns packed with SPPs can be larger than 2. In addition, the h_{min} of sub-2-μm SPPs can be larger than that of sub-3-μm SPPs and column performance can be substantially affected by the packing conditions [76]. Due to the increasing popularity of narrow-bore columns for many reasons (e.g. LC/MS and greener chromatogra-

phy), there is a strong need for more efficient packing of small SPPs into narrow-bore columns to help realize the full potential of these particles.

5.3. New phase chemistries for wider selectivity

The new particle technology of modern SPPs brings impressive chromatographic efficiency. The next step is naturally to manipulate phase chemistry on this platform to achieve a wide selection of selectivity. This trend is already clear in recent conferences such as Pittcon 2011, where column manufacturers started to offer new phases [3]. This trend should continue until the next breakthrough in particle technology.

6. Conclusions

Modern superficially porous particles are quickly gaining popularity due to their impressive chromatographic efficiency. This is especially true for the sub-3-μm SPPs because they offer much improved reduced plate height and lower backpressure compared to the sub-2-μm totally porous particles. In this review, we use optimization theory to compare the performance of sub-3-μm SPPs, sub-2-μm SPPs, sub-2-μm totally porous particles and traditional totally porous particles. When we use the three-parameter optimization to assess their *performance potential*, we discover that the sub-3-μm SPP (albeit at lower pressure of 600 bar) will always provide the best separation performance. When we conduct the more practically relevant two-parameter optimization, we learn that the 2.7 μm SPPs give superior performance over the other three particles in a very wide analysis time range, i.e. when column dead time is longer than about 30 s (or analysis time longer than 3 min). In addition, this advantage increases as analysis time increases.

Successful examples of applying modern SPPs in different application areas are reviewed, according to the required speed and efficiency. It is evident that SPPs provide good solutions over a wide range of sample complexity and analysis time. Examples range from ultrafast separations within a minute, to common separations of about 10 min, to ultrahigh resolution separation lasting several hours. With active and continuous effort to develop better SPPs, more exciting development and applications of SPPs are yet to be seen.

Acknowledgements

The authors would like to thank Professor Nobuo Tanaka for his invitation to write this review. We thank Professors Peter Carr and Dwight Stoll for insightful discussions and comments. Ron Majors, Maureen Joseph, Jason Link, Anne Mack and Monika Dittmann are also acknowledged for many helpful discussions.

References

[1] C.G. Horvath, B.A. Preiss, S.R. Lipsky, Anal. Chem. 39 (1967) 1422.
[2] G. Guiochon, F. Gritti, J. Chromatogr. A 1218 (2011) 1915–1938.
[3] R. Majors, LC–GC North Am. 29 (2011) 218.
[4] R. Majors, LC–GC North Am. 28 (2010) 932.
[5] M. Dong, D. Yazzie, N.P. Chetwyn, Proceedings of the Pittsburgh Conference, Atlanta, GA, March 13–17, 2011.
[6] J.H. Knox, M. Saleem, J. Chromatogr. Sci. 7 (1969) 614.
[7] W. Stober, A. Fink, E. Bohn, J. Colloid Interface Sci. 26 (1968) 62.
[8] F. Gritti, A. Cavazzini, N. Marchetti, G. Guiochon, J. Chromatogr. A 1157 (2007) 289.
[9] F. Gritti, I. Leonardis, D. Shock, P. Stevenson, A. Shalliker, G. Guiochon, J. Chromatogr. A 1217 (2010) 1589.
[10] D. Cabooter, A. Fanigliulo, G. Bellazzi, B. Allieri, A. Rottigni, G. Desmet, J. Chromatogr. A 1217 (2010) 7074.
[11] C. Dewaele, M. Verzele, J. Chromatogr. 260 (1983) 13.
[12] J. Billen, D. Guillarme, S. Rudaz, J.L. Venthey, H. Ritchie, B. Grady, G. Desmet, J. Chromatogr. A. 1161 (2007) 224.
[13] S.A. Schuster, B.M. Wagner, B.E. Boyes, J.J. Kirkland, J. Chromatogr. Sci. 48 (2010) 566.
[14] F. Gritti, G. Guiochon, J. Chromatogr. A 1218 (2011) 907.
[15] F. Gritti, I. Leonardis, J. Abia, G. Guiochon, J. Chromatogr. A 1217 (2010) 3819.
[16] F. Gritti, G. Guiochon, J. Chromatogr. A 1217 (2010) 5137.
[17] F. Gritti, G. Guiochon, J. Chromatogr. A 1218 (2011) 1592.
[18] X. Wang, W.E. Barber, P.W. Carr, J. Chromatogr. A 1107 (2006) 139.
[19] Y. Zhang, X. Wang, P. Mukherjee, P. Petersson, J. Chromatogr. A 1216 (2009) 4597.
[20] G. Desmet, S. Deridder, J. Chromatogr. A 1218 (2011) 32.
[21] S. Deridder, G. Desmet, J. Chromatogr. A 1218 (2011) 46.
[22] J.M. Cunliffe, T.D. Maloney, J. Sep. Sci. 30 (2007) 3104.
[23] D. Cabooter, F. Lestremau, F. Lynen, P. Sandra, G. Desmet, J. Chromatogr. A 1212 (2008) 23.
[24] P.W. Carr, X. Wang, D.R. Stoll, Anal. Chem. 81 (2009) 5342.
[25] H. Poppe, J. Chromatogr. A 778 (1997) 3.
[26] G. Desmet, D. Clicq, P. Gzil, Anal. Chem. 77 (2005) 4058.
[27] G. Guiochon, J. Chromatogr. A 1168 (2007) 101.
[28] R.W. Brice, X. Zhang, L.A. Colon, J. Sep. Sci. 32 (2009) 2723.
[29] D.V. McCalley, J. Chromatogr. A 1217 (2010) 4561.
[30] X. Wang, P.W. Carr, D.R. Stoll, LC–GC North Am. 28 (2010) 932.
[31] G. Desmet, P. Gzil, D. Clicq, LC–GC Eur. 18 (2005) 403.
[32] D.V. McCalley, J. Chromatogr. A 1218 (2011) 2887.
[33] J. Ding, C.M. Sorensen, Q. Zhang, H. Jiang, N. Jaitly, E.A. Liversay, Y. Shen, R.D. Smith, T.O. Metz, Anal. Chem. 79 (2007) 6081.
[34] G. Desmet, D. Clicq, D.T.T. Nguyen, D. Guillarme, S. Rudaz, J.L. Veuthey, N. Vervoort, G. Torok, D. Cabooter, P. Gzil, Anal. Chem. 78 (2006) 2150.
[35] D. Cabooter, G. Desmet, F. Lestremau, Proceedings of the HPLC 2010, Boston, MA, June 14–19, 2010.
[36] D.N. Mallett, C. Ramirez-Molina, J. Pharm. Biomed. Anal. 49 (2009) 100.
[37] J.M. Cunliffe, C.F. Noren, R.N. Hayes, R.P. Clement, J.X. Shen, J. Pharm. Biomed. Anal. 50 (2009) 46.
[38] J.M. Cunliffe, J.X. Shen, X. Wei, D.P. Dreyer, R.N. Hayes, R.P. Clement, Bioanalysis 3 (2011) 735.
[39] E.R. Badman, R.L. Beardsley, Z. Liang, S. Bansal, J. Chromatogr. B 878 (2010) 2307.
[40] W. Song, D. Pabbisetty, E.A. Groeber, R.C. Steenwyk, D.M. Fast, J. Pharm. Biomed. Anal. 50 (2009) 491.
[41] Y.W. Alelyunas, L. Pelosi-Kilby, P. Turcotte, M. Kary, R.C. Spreen, J. Chromatogr. A 1217 (2010) 1950.
[42] D.R. Stoll, X. Li, X. Wang, P.W. Carr, S.E.G. Porter, S.C. Rutan, J. Chromatogr. A 1168 (2007) 3.
[43] R.E. Murphy, M.R. Schure, J.P. Foley, Anal. Chem. 70 (1998) 1585.
[44] S.R. Groskreutz, M.M. Swenson, L.B. Secor, D.R. Stoll, J. Chromatogr. A (2011), doi:10.1016/j.chroma.2011.06.035.
[45] P.W. Carr, D.R. Stoll, X. Wang, Anal. Chem. 83 (2011) 1890.
[46] A.J. Alexander, L. Ma, J. Chromatogr. A 1216 (2009) 1338.
[47] P. Yang, G.R. Litwinski, M. Pursch, T. McCabe, K. Kuppannan, J. Sep. Sci. 32 (2009) 1816.
[48] S. Fekete, J. Fekete, Talanta 84 (2011) 416.
[49] A. Abrahim, M. Al-Sayah, P. Skrdla, Y. Bereznitski, Y. Chen, N. Wu, J. Pharm. Biomed. Anal. 51 (2010) 131.
[50] A. Gratzfeld-Hüsgen, E. Naegele, Application Note 5990-5602EN, Agilent Technologies, Inc., 2010.
[51] D.V. McCalley, J. Chromatogr. A 1193 (2008) 85.
[52] J.J. Kirkland, J. Chromatogr. Sci. 7 (1969) 7.
[53] C. Horvath, S.R. Lipsky, J. Chromatogr. Sci. 7 (1969) 109.
[54] J.J. Kirkland, US Patent 3,505,785 (1969).
[55] J.J. Kirkland, Anal. Chem. 41 (1969) 218.
[56] J.J. Kirkland, F.A. Truszkowski, C.H. Dilks, G.S. Engel, J. Chromatogr. A 890 (2000) 3.
[57] J.J. Kirkland, F.A. Truszkowski, R.D. Ricker, J. Chromatogr. A 965 (2002) 25.
[58] R.D. Ricker, C.B. Woodward III, K. Forrer, B.J. Permar, W. Chen, J. Chromatogr. Sci. 46 (2008) 261.
[59] Q. Wang, N.A. Lacher, B.K. Muralidhara, M.R. Schlittler, S. Aykent, C.W. Demarest, J. Sep. Sci. 33 (2010) 2671.
[60] G. Guiochon, in: C. Horvath (Ed.), High-Performance Liquid Chromatography: Advances and Perspectives, vol. 2, Academic Press, New York, 1980, p. 1.
[61] F. Gritti, C.A. Sanchez, T. Farkas, G. Guiochon, J. Chromatogr. A 1217 (2010) 3000.
[62] F. Gritti, G. Guiochon, J. Chromatogr. A 1217 (2010) 7677.
[63] K.J. Fountain, U.D. Neue, E.S. Grumbach, D.M. Diehl, J. Chromatogr. A 1216 (2009) 5979.
[64] F. Gritti, G. Guiochon, J. Chromatogr. A 1218 (2011) 4632.
[65] S. Heinisch, G. Desmet, D. Clicq, J.L. Rocca, J. Chromatogr. A 1203 (2008) 124.
[66] J. Dai, P.W. Carr, D.V. McCalley, J. Chromatogr. A 1216 (2009) 2474.
[67] F. Gritti, G. Guiochon, J. Chromatogr. A 1176 (2007) 107.
[68] J. Zheng, D. Patel, Q. Tang, R.J. Markovich, A.M. Rustum, J. Pharm. Biomed. Anal. 50 (2009) 815.
[69] P.C. Iraneta, K.D. Wyndham, D.R. McCabe, T.H. Walter, Charged Surface Hybrid Technology White Paper, Waters Corporation, 2010.
[70] R. Majors, LC–GC North Am. 29 (2011) 476.

[71] U.D. Neue, D. McCabe, V. Ramesh, H. Pappa, J. DeMuth, Pharmacopeial Forum 35 (2009) 1622.
[72] L.R. Snyder, J.W. Dolan, High-Performance Gradient Elution, John Wiley & Sons, Hoboken, NJ, 2007.
[73] K. Horvath, F. Gritti, J.N. Fairchild, G. Guiochon, J. Chromatogr. A 1217 (2010) 6373.
[74] J.O. Omamogho, J.P. Hanrahan, J. Tobin, J.D. Glennon, J. Chromatogr. A 1218 (2011) 1942.
[75] F. Gritti, G. Guiochon, J. Chromatogr. A 1217 (2010) 8167.
[76] L.E. Blue, J.W. Jorgenson, Proceedings of the Pittsburgh Conference, Atlanta, GA, March 13–17, 2011.